B1 cells produce anti-phosphatidylserine antibodies via TLR-mediated Syk activation and contribute to lupus nephritis development

Supplementary Table and Figures

Supplementary Table 1. Patient and heathy control characteristics

		SLE		
	HC (n=18)	PS-specific IgG Low (n=29)	PS-specific IgG High (n=35)	Statistics
Cohort demographics				
Female (%)	17/18	29/29	34/35	-
Mean age (years)	30.7 ± 6.7	31.0± 13.8	38.6 ± 13.9	p = 0.0224 *
Patient characteristics				
SLEDAI	/	5.4 ± 3.0	8.5 ± 6.8	p = 0.0351 *
Nephritis	/	7/22	15/20	
Disease duration (years)	/	3.8 ± 3.3	7.6 ± 7.3	.p = 0.0462 *
Laboratory parameters				
Anti-dsDNA (IU/mL)	/	119.9 ± 142.7	711.7 ± 865.3	p < 0.0001 ****
C3 (d/L)	/	0.68 ± 0.27	0.63 ± 0.28	n.s
C4 (d/L)	/	0.14 ± 0.09	0.37 ± 1.5	n.s
WBC (10^9/L)	/	6.3 ± 3.2	6.3 ± 2.6	n.s
PLT (10^9/L)	/	172.3± 69.2	221.5 ± 124.9	n.s
RBC (10^{12}/L)	/	3.7 ± 0.8	3.8 ± 0.8	n.s.

Data are presented as mean ± SEM according to data distribution. Groups were compared with *Mann-Whitney U test (between two groups). HC, healthy controls; SLE, Systemic Lupus Erythematosus; Anti-PS IgG Low ($Absorbance_{OD450nm} < 1$); Anti-PS IgG positive ($Absorbance_{OD450nm} > 1$); SLEDAI, Systemic Lupus Erythematosus Disease Activity Index; C, complement factor; WBC, white blood cell; PLT, platelet; RBC, red blood cell.

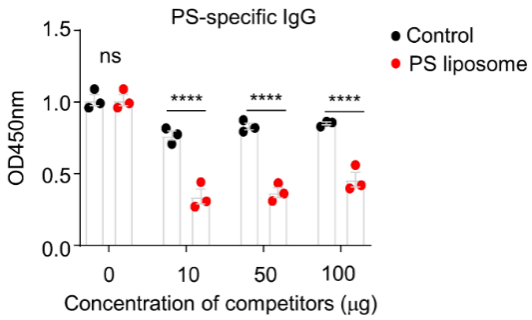

Supplementary Fig. 1 SLE PS-specific IgG effectively binding to the PS liposome with high affinity. Data plot shows the serum PS-specific IgG levels with active SLE serum (SLEDAI > 5, n = 3) by the competitive ELISA assay with preincubation PS antigen (PS liposome) or control antigen (PC liposome) for 1 h. Nonparametric Mann–Whitney *U* test, ****, P <0.0001.

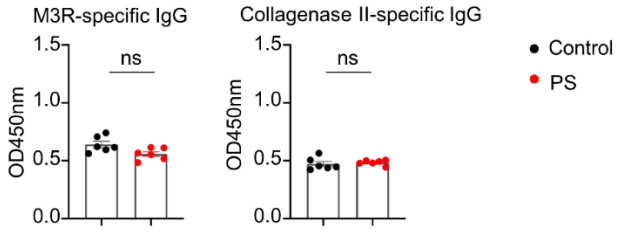

Supplementary Fig. 2 Comparable levels of M3R- or collagenase II- specific IgG in mice with PS liposome immunization. Representative data plots show M3R-specific IgG (αM3R IgG) and collagenase II -specific IgG (αcollagenase II IgG) in serum samples (1:200 dilution) of control or PS immunized mice for 12 weeks (n = 6 per group). Unpaired two-tailed Student's t-test, ns, no significance.

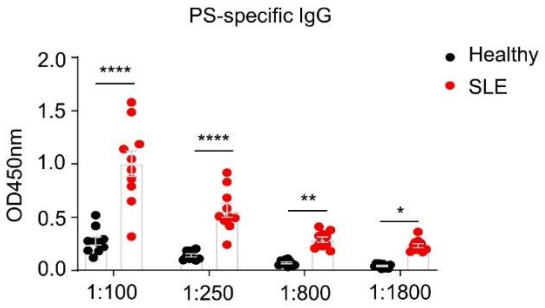

Supplementary Fig. 3 Elevated levels of serum PS-specific IgG in SLE patients. Data plot shows the serum PS-specific IgG levels using gradient diluted serum samples (1:100, 1:250, 1:800 and 1:1800) from active SLE patients (SLEDAI > 5, n =10) and healthy donors (n = 10). Nonparametric Mann–Whitney *U* test, *, $P < 0.05$; **, $P < 0.01$; ****, $P < 0.0001$.

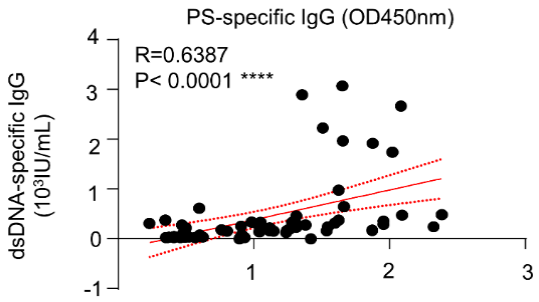

Supplementary Fig. 4 Positive correlation between serum levels of PS-specific IgG and dsDNA-specific IgG in SLE patients. Data plot shows the correlation between serum PS-specific IgG levels and dsDNA-specific IgG in SLE patients (n = 64). Spearman's rank coefficient of correlation, ****, P <0.0001.

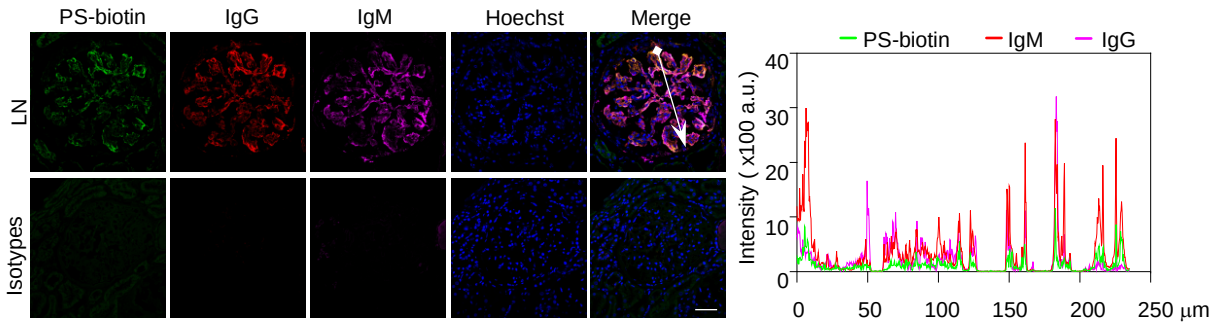

Supplementary Fig. 5 Renal deposition of PS-reactive autoantibodies in patients with LN. Representative confocal images show the colocalization of PS-biotin (detected with Alex fluo 488-streptavidin), IgG and IgM in kidney biopsies of lupus nephritis patients (scale bar, 50μm).

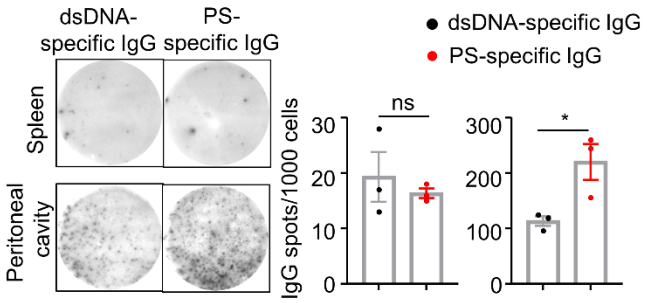

Supplementary Fig. 6 Peritoneal B cells are the major source of PS-specific IgG in lupus mice. Representative ELISPOT detections and data plots show the PS-specific and dsDNA-specific IgG spots in splenic and peritoneal B cells from lupus mice (n = 3). Unpaired two-tailed Student's t-test, ns, no significance; *, $P < 0.05$.

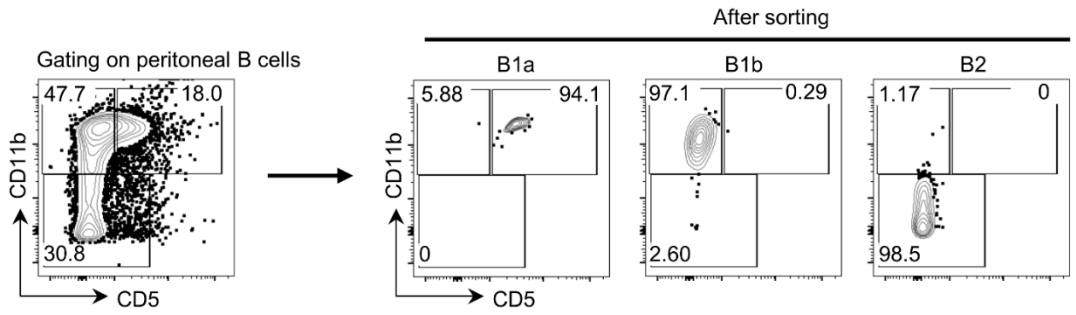

Supplementary Fig. 7 Sorting purity of B cell subsets. Representative flow cytometric images show the frequencies of peritoneal B1a, B1b, and B2 cells before and after cell sorting.

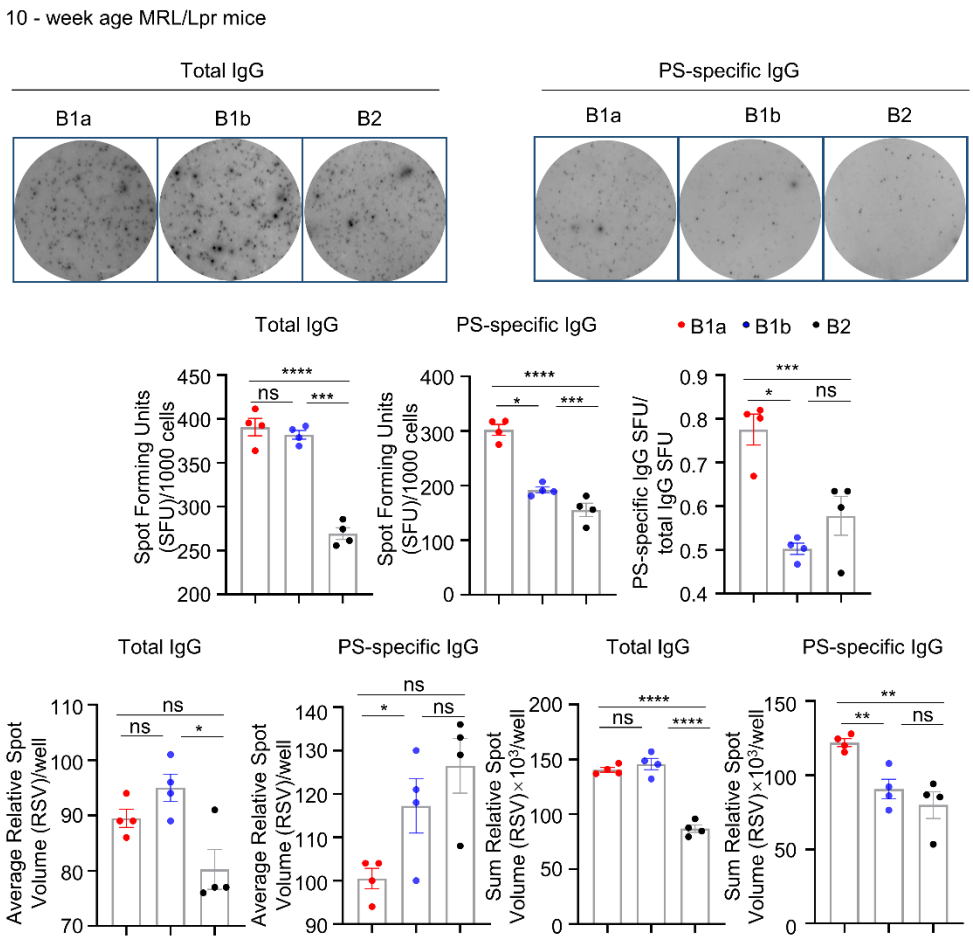

Supplementary Fig. 8 ELISPOT analysis of peritoneal B cell subsets in MRL/Lpr mice. B1a, B1b and B2 cells were sorted and purified from peritoneal cavity of MRL/Lpr mice at 10 weeks of age. Total IgG and PS-specific IgG-secreting cells were detected by ELISPOT assay. The Spot Forming Units (SFU) of total IgG and PS-specific IgG spot, total IgG/PS-specific IgG spot SFU ratio, average and sum Relative Spot Volume (RSV) of by total IgG and PS-specific IgG spots an IRIS reader. n = 4 per group. Unpaired t-test; ns, no significance; *, p <0.05; **, p<0.01; ***, p<0.001; ****, p <0.0001.

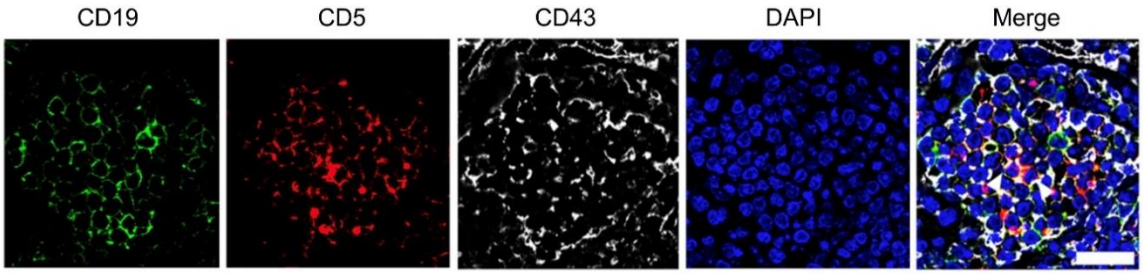

Supplementary Fig. 9 Renal infiltration of B1 cells in lupus mice. Representative confocal image shows CD43(white), CD5(red), and CD19 (green) triple-positive B1a cells in kidney sections of 24-week-old MRL/Lpr mice (scale bar, 20μm).

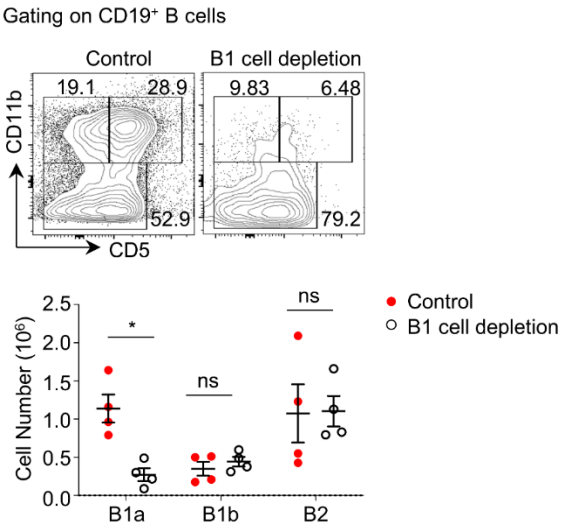

Supplementary Fig. 10 Efficacy of B1a depletion in MRL/Lpr mice. Representative flow cytometric profiles and data plot show B1a cells, B1b cells and B2 cells in peritoneal cavity of MRL/Lpr mice with control PBS or hypo-osmotic water treatment for successive 20 weeks (n = 4 per group). Unpaired two-tailed Student's t-test, ***, $P < 0.001$.

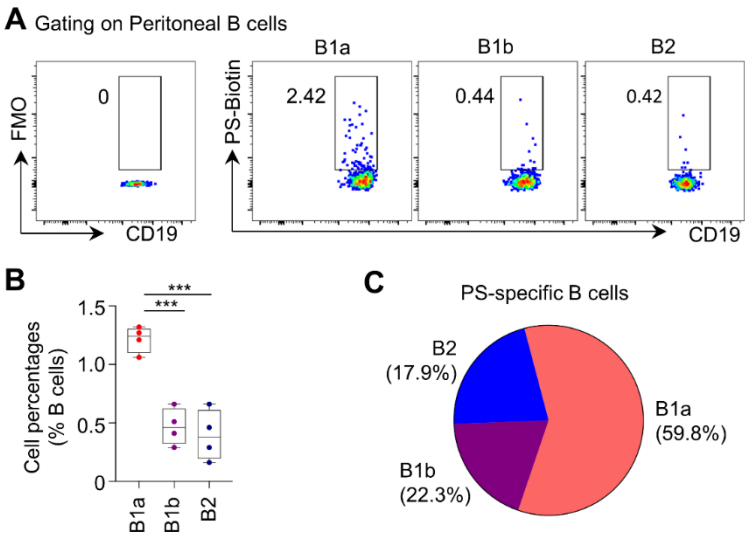

Supplementary Fig.11 B1a cells are the major compartment of PS-specific B subsets in lupus-prone MRL/Lpr mice. (A-C) Representative flow cytometric profiles (A), the data plot (B) and pie chart (C) show PS-specific B subsets within B1a cells, B1b cells and B2 cells in peritoneal cavity of MRL/Lpr mice at 24-week age (n = 3). One-way ANOVA, ***, $P < 0.001$.